Nano-Fe^0 Immobilized onto Functionalized Biochar Gaining Excellent Stability during Sorption and Reduction of Chloramphenicol via Transforming to Reusable Magnetic Composite

Mohammad B. Ahmed, John L. Zhou, Huu H. Ngo, Wenshan Guo, Md A.H. Johir, Kireesan Sornalingam, Dalel Belhaj, Monem Kallel

PII: S1385-8947(17)30607-1
DOI: http://dx.doi.org/10.1016/j.cej.2017.04.063
Reference: CEJ 16817

To appear in: *Chemical Engineering Journal*

Received Date: 15 February 2017
Revised Date: 11 April 2017
Accepted Date: 12 April 2017

Please cite this article as: M.B. Ahmed, J.L. Zhou, H.H. Ngo, W. Guo, M.A.H. Johir, K. Sornalingam, D. Belhaj, M. Kallel, Nano-Fe^0 Immobilized onto Functionalized Biochar Gaining Excellent Stability during Sorption and Reduction of Chloramphenicol via Transforming to Reusable Magnetic Composite, *Chemical Engineering Journal* (2017), doi: http://dx.doi.org/10.1016/j.cej.2017.04.063

Nano-Fe^0 Immobilized onto Functionalized Biochar Gaining Excellent Stability during Sorption and Reduction of Chloramphenicol via Transforming to Reusable Magnetic Composite

Mohammad B. Ahmed[a], John L. Zhou[a]*, Huu H. Ngo[a], Wenshan Guo[a], Md A.H. Johir[a], Kireesan Sornalingam[a], Dalel Belhaj[b], Monem Kallel[b]

[a]School of Civil and Environmental Engineering, University of Technology Sydney, 15 Broadway, NSW 2007, Australia

[b]ENIS, Engineering Laboratory of Environment and Ecotechnology, LR16ES19, University of Sfax, Sfax, Tunisia

Corresponding author

Prof John L Zhou

School of Civil and Environmental Engineering

University of Technology Sydney

15 Broadway, NSW 2007

Australia

Email: junliang.zhou@uts.edu.au

Abstract

The widely used nanosized zero-valent iron (nZVI or nFe^0) particles and their composite material lose reductive nature during application, and the stability of transformed composite material for repeatable application is not addressed to date. To shed light on this, nZVI was synthesized from scrap material and immobilized on functionalized biochar (fBC) to prepare nZVI-fBC composite. Comparative study between nZVI and nZVI-fBC composite on the removal of chlorinated antibiotic chloramphenicol from different water types was conducted. The results suggested that nZVI was solely responsible for reduction. Whereas nZVI-fBC could be applied once, within a few hours, for the reduction (29-32.5%) and subsequently sorption (67.5-70.5%) by transforming to a fully magnetic composite (nFe_3O_4-fBC) gaining stability and synergistic sorption performance. In both cases, two reduction by-products were identified namely 2-chloro-N-[1,3-dihydroxy-1-(4-aminophenyl)propan-2-yl]acetamide (*m/z* 257) and dechlorinated N-[1,3-dihydroxy-1-(4-aminophenyl)propan-2-yl]acetamide (*m/z* 223). The complete removal of 3.1 μM L^{-1} of chloramphenicol in different water was faster by nZVI-fBC (~12-15 h) than by stable nFe_3O_4-fBC composite (~18 h). Both nZVI-fBC and nFe_3O_4-fBC composites removed chloramphenicol in the order: deionized water > lake water > synthetic wastewater. nFe_3O_4-fBC showed excellent reusability after regeneration, with the regenerated nFe_3O_4-fBC (after 6 cycles application) showing significant performance for methylene blue removal (~287 mg g^{-1}). Therefore, the transformed nFe_3O_4-fBC composite is a promising and reusable sorbent for the efficient removal of organic contaminants.

Keywords: Functionalized biochar; Dechlorination; nZVI-fBC; nFe_3O_4-fBC; Magnetic composite; Antibiotic

1. Introduction

In the last two decades, many studies have demonstrated that ZVI (redox potential, E^o = -0.44 V) and several other zero-valent metals (e.g. Sn^0, Zn^0, Al^0 and Mn^0) can serve as efficient reducing agents for the remediation of chlorinated organic compounds, nitro-aromatic compounds, heavy metals, nitrate, dyes and phenolic compounds from groundwater and wastewater [1-8]. ZVI is non-toxic, abundant, cheap and easy to produce, and its reduction process requires little maintenance [5]. To date, most of the studies have focused on using ZVI to remove chlorinated hydrocarbons from water [4, 9-11] due to dechlorinative reduction nature of ZVI. However, ZVI can be easily oxidized in the presence of oxygen. Powder state unstable nanosized ZVI and its intrinsic characteristics to react with surrounding media or agglomerate during preparatory processes as well as during application hinder its direct application and reduce its reactivity with poor mobility and transport for the continuous *in situ* environmental remediation [12]. These phenomena leading to ZVI applications in fixed bed column or other dynamic flow systems result in high-pressure drop and restriction of nZVI for field scale applications [12]. Attempts have been proposed to enhance the nZVI transport in natural subsurface environments with common objective of stabilizing the colloidal suspensions. nZVI has already been coated/impregnated with polymeric materials (such as polystyrene sulfonate, polyacrylic acid, carboxymethylcellulose), combined with resin, biochar [13], activated carbon [14, 15], multi-walled carbon nanotube [16], clay mineral supported (kaolinite, zeolite, clay, montmorillonite, rectorite, palygorskite, and bentonite) [17-22], and modified with hydrophilic carbon, and embedded in a silica matrix to obtain a stable nZVI suspension [23]. It was reported that nZVI particles modified by covalently binding with carboxymethylcellulose exhibited high transport potential in packed beds of glass, beads, sand and soil [23]. All these research reported that nZVI-composites materials were applied once for contaminant removal, with repetitive applications being rare. In addition, the fate of these nZVI-composites for further stage of application in repeatable

manner is not clear. Theoretically and practically, nZVI particles in composite materials lose their reductive nature during application when in contact with the contaminants and eventually produce different species either in solution or in composite by releasing and reacting loosely bonded surface ZVI and along in composite surface. The questions that arise are: what is the transformed ZVI-composite material? Is it stable and useable for further and repetitive applications? What are its unique characteristics in terms of chemical structure and interfacial properties? Thus to shed light on nZVI and its composite, we have synthesized nZVI from scrap materials and immobilized on functionalized biochar (fBC), which were tested for the removal of a chlorinated antibiotic chloramphenicol [(2,2-dichloro-N-[1,3-dihydroxy-1-(4-nitrophenyl)propan-2-yl]acetamide)] over repetitive cycles.

Of global concern today are antibiotics that are widely manufactured and used to treat the diseases caused by microorganisms. They are unique as they can selectively act on bacteria and pathogens by leaving the human cells and tissues unchanged, but prolonged exposure to antibiotics may develop antibiotic resistance genes [24-28]. Chloramphenicol as an antibiotic can cause geno-toxic and other side effects such as aplastic agranulocytosis, anaemia, and leukopenia [28]. Low removal efficiencies of chloramphenicol from wastewater has been reported using biological treatment technologies as it does not degrade in the metabolic system and thus, has been frequently detected in surface water, groundwater, and even in drinking water [25, 29]. The removal of chloramphenicol from wastewater has been reported using different physicochemical methods [10, 30, 31], among which ZVI has been widely applied [9-11]. Moreover, different studies reported different reduction products [9-11, 28], and so far no study has been conducted using ZVI and ZVI-carbonaceous composite for removing chloramphenicol except from deionized water. Hence, the application of ZVI and its composite for removing chloramphenicol from different water and the identification of byproducts are of great importance. In addition, such kind of composite may possess simultaneous sorption and reduction which has not been reported. Thus the calculation of the

amount of sorption and reduction is necessary to differentiate the role of each in such composite materials.

Therefore, this study aimed to use nZVI-fBC as well as ZVI (for comparative purpose) with emphasizing given on the stability of nZVI-fBC composite along with focusing on the transformed magnetic composite (i.e. nFe_3O_4-fBC) for repeatable applications. In addition, the role of nZVI and nZVI-fBC composite for the reductive dechlorination and sorption of chloramphenicol with detailed mechanisms was investigated. Furthermore, the reduced products of chloramphenicol using nZVI and nZVI-fBC composite were identified. The effect of regeneration of the magnetized composite for repeatable application for chloramphenicol removal was assessed up to six cycles. Finally, nFe_3O_4-fBC composite was applied (6 cycles of application) for the removal of methylene blue to assess its suitability for reuse.

2. Materials and methods

2.1. Chemicals and sorbent

The standards of chloramphenicol, methylene blue and organic solvents (methanol, acetonitrile, formic acid) of HPLC grade were purchased from Sigma-Aldrich, Australia. Humic acid, tannic acid, arabic acid, acacia gum powder, ammonium sulphate, beef extract, peptone, sodium lignin sulphonate, Na-laryl sulphate, K_2HPO_4, ammonium bicarbonate, magnesium sulphate, potassium chloride, sulphuric acid (~98%), nitric acid (~68), and sodium borohydrate ($NaBH_4$) were of analytical-grade. Iron oxide (Fe_3O_4) nano particles (<50 nm) were also purchased from Sigma Aldrich.

Eucalyptus globulus wood derived biochar was prepared by heating the wood particles at 380 ^oC for 2 h in a reactor under continuous nitrogen gas supply and functionalization of this biochar was carried out according to previous method [32]. Biochar and fBC were used for the sorption of chloramphenicol. Based on preliminary experiments it was found that fBC was much more effective for the immobilization of ZVI than biochar itself. Hence fBC was

chosen for the nZVI-fBC composite preparation for the maximum immobilization of ZVI on fBC surface. fBC (75 μm to 1.0 mm) is the biochar containing different functional groups such as –COOH, -OH, C=O and C=C on its surface.

2.2. nZVI synthesis and preparation of nZVI-fBC composite

Scrap iron waste (a mixture of iron material and plastics) collected from UTS engineering workshop was washed several times with tap water. The scrap iron material (30 g) was mixed with 120 mL of 10% HNO_3 for 10 min to remove impurities. The residual iron material was transferred to 600 mL of 15% H_2SO_4 (v/v) and stirred for 3 h at 60 ^{0}C. The residues were separated by settling. This ferrous sulphate solution (green color) was obtained by filtration and stored as stock solution for further use. The stock solution iron concentration was measured and found iron concentration being 21.9 g L^{-1}.

The stock solution (15 mL) was diluted 10 times with deionized water and pH was adjusted to ~5.0 using 2 M NaOH solution. Thus, ferrous sulphate was transformed to reddish brown ferric sulphate and stirred for few minutes. Then, 15 mL of 1.6 M $NaBH_4$ was added drop-wise into the solution and mixed vigorously for 30 min and nZVI was produced (**equation 1**). The nZVI solution was centrifuged at 2000 rpm for 7 min and washed with ethanol. Finally, nZVI was dried in a vacuum oven for 8 h and stored in airtight container till further use.

$$4Fe^{3+} + 3BH_4^- + 9H_2O \rightarrow 4Fe^0 + 3H_2BO_3^- + 6H_2 + 12H^+ \quad (1)$$

To produce nZVI-fBC composite, 5 mL of the stock solution was diluted ten times and pH was adjusted to 5.0 using 2 M NaOH and mixed thoroughly for 5 min. Then 1.0 g of fBC was added to the solution and mixed for 2 h and 5 mL of ethanol was added. Next, 5 mL of 1.6 M $NaBH_4$ was added drop-wise into the solution and mixed vigorously for another 2 h. Thus, nZVI was immobilized onto fBC surface. Finally the product was filtered, washed, dried and stored to obtain nZVI-fBC composite.

2.3. Sorption experiments, analysis and data fittings

The interactions of biochar, fBC, nZVI, nZVI-fBC composite, and nFe_3O_4-fBC composite i.e. magnetic-fBC (converted composite during chloramphenicol removal and regeneration) with chloramphenicol solution were carried out at pH 4.0-4.5, 25 ^oC, based on previous study [10], in order to get maximum removal of chloramphenicol. nZVI, nZVI-fBC and magnetic-fBC were applied in different water types to determine their sorption and reduction nature of chloramphenicol. The supernatant concentration was measured using HPLC (Jasco) with aliquots from each reactor being taken and filtered through a 0.2 μm PTFE filter followed by 50 μL of sample injection. HPLC equipped with an auto-sampler, a UV detector at 285 nm, and a Zorbax Bonus RP C_{18} column (5.0 μm, 2.1 ×1.50 mm, Agilent Technologies) was used for separation. Mobile phase A was composed of acetonitrile and formic acid (99.9: 0.1) while mobile phase B was composed of Milli-Q water and formic acid (99.9: 0.1). The elution used 40% of A and 60% of B at a flow rate of 0.4 mL min^{-1}, which was changed to 0.3 mL min^{-1} at 0.1 min. The method was run over 7 min.

Chloramphenicol and its reduced products were identified by LC-MS/QTOF in positive mode, on an Agilent Poroshell 120 EC-C_{18} column (2.7 μm, 4.6 mm x 50 mm). The elution began with 95% pure water and 5% methanol, ending with 1% pure water and 99% methanol within 9 min at a flow rate of 0.35 mL min^{-1}. Following elution, the mobile phase was changed to 95% water and 5% methanol. The total run time was 13 min.

Stock solution of methylene blue (1.0 g L^{-1}) was diluted to different initial concentrations. The nFe_3O_4-fBC composite was added without adjustment of the solution pH at a dosage of 0.5 g L^{-1} for methylene blue solution. The mixture was shaken on an orbital shaker at 120 rpm for 24 h at 25 ^oC. The methylene blue concentration was measured by UV-visible spectroscopy (Shimadzu). The sorption capacities of biochar, fBC, nFe_3O_4 and nFe_3O_4-fBC for chloramphenicol and methylene blue were calculated, and modelled using the Langmuir and Freundlich isotherms (details in supporting information).

2.4. Characterizations of fBC, nZVI, nZVI-fBC and nFe_3O_4-fBC composite

Scanning electron microscopy (SEM) with energy dispersive spectrometer (EDS) was used to determine the morphological and chemical composition of the materials (Zeiss Evo-SEM). XRD analysis of the samples was carried out using a Bruker D8 Discover diffractometer using CuKα radiation, in the scattering angle 2θ range 20^o-60^o. Fourier transform infrared spectroscopy (FTIR) (Miracle-10: Shimadzu) was used to determine surface functional groups. The spectra were obtained at 4 cm^{-1} resolution by measuring the absorbance from 400 to 4000 cm^{-1} using a combined 40 scans. Raman shifts measurement was carried out using Renishaw in via Raman spectrometer (Gloucestershire, UK) equipped with a 17 mW Renishaw Helium-Neon Laser 633 nm and CCD array detector using 50% laser intensity. The abundance of surface functional groups on nZVI-fBC was obtained by using X-Ray Photoelectron Spectroscopy (XPS) (Thermoscientific, UK). Iron concentration was determined using microwave plasma atomic emission spectroscopy (4100-MP-AES, Agilent Technologies). Zeta potential values of nZVI and nFe_3O_4-fBC composite were measured with 0.1 M KCl solution using a Nano-ZS Zeta-seizer (Malvern, Model: ZEN3600). Zeta potential values were measured at different pH values (**Table A2**). Particle size distribution of nZVI was also measured using the same instrument.

2.5. Comparative study in different water types

Lake surface water (pH 7.2, temperature 19.9 ^oC, total dissolved solids 116 mg L^{-1}, total organic carbon 75.56 mg L^{-1}, total carbon 76.72 mg L^{-1}) was collected from the Victoria Park, NSW, Australia and was filtered through 1.2 μm filter paper before being stored at 4 ^oC. Synthetic wastewater was prepared based on a recent study [33] (**Table A3**). Deionized water, lake surface water and synthetic wastewater were spiked with 3.10 μM L^{-1} of chloramphenicol before contact with nZVI, nZVI-fBC and magnetic-fBC composite to assess the extent of sorption in different water types.

2.6. Desorption and regeneration of magnetic-fBC composite

Desorption of chloramphenicol was carried out to calculate and differentiate the reduction and sorption percentage of chloramphenicol using nZVI-fBC (after application in the 1st cycle) and magnetic-fBC composite (2nd to further cycles). After experiments, the supernatant was decanted and replaced with an equal volume of 50% methanol solution as solvent (solvent regeneration). After 24 h, the suspension was centrifuged for 7 min at 2000 rpm and chloramphenicol concentration was measured directly by HPLC. Desorption was performed up to 2nd cycle. The thermal regeneration of magnetic-fBC (after 1st cycle application, nZVI-fBC transformed to magnetic-fBC composite) was carried out in an oven by heating at a pre-set temperature 300 ^{o}C for 1 h.

3. Results and discussion

3.1. Material structure and composition

The morphologies of nZVI, nZVI-fBC composite, and nFe_3O_4-fBC composite were analysed by SEM, EDS, XRD, XPS and Raman spectra. SEM images of unsupported fBC, nZVI-fBC and magnetic-fBC composite are shown in **Figs 1 and A1**. In the case of nZVI-fBC, the fBC surface was partially covered by the loaded nZVI particles (**Fig. 1b**) and appeared to be uneven whereas bare fBC surface was smooth in appearance (**Fig. 1a**). Even after six cycles of application the SEM image (**Fig. 1c**) shows the presence of nanosized iron oxide particles on fBC surface indicating that iron oxide particles were successfully incorporated with fBC by forming a stable magnetic-fBC composite. It also found some portion of nZVI in nZVI-fBC composite was loosely bonded with fBC surface, which was confirmed by the analysis of iron content in nZVI-fBC. The iron content in the nZVI-fBC composite (7.8%) was determined by digesting of the composite in nitric acid solution (3%, v/v) followed by MP-AES analysis. In order to validate the composition of iron oxides formed on nZVI-fBC, EDS

analysis was performed with nZVI-fBC composite (**Table A1)** and ~8.3% iron content was obtained.

XRD studies of nZVI showed the crystalline domain size of ZVI nanoparticles **(Fig. 1d).** The crystalline scattering domain size of nFe^o was found at $2\theta = 45^o$ and 28^o [7]. Particle size distribution data showed that nZVI had particle sizes in the range of 220.2 nm (77.9 %) and 190.1 nm (22.1%). In addition, iron oxide was also present in ZVI due to the oxidation of a small portion of nZVI during measurement, preparatory processes or even in drying processes. EDS data showed that nZVI comprised around 92-95% of nFe^o with the rest being oxidized to $FeOOH/Fe_2O_3/Fe_3O_4$ particles (**Table A1 and Fig. A2**). XPS analysis of nZVI-fBC showed that C1s spectra surface of this composite composed of aromatic carbon in the form of C=C (284.4 eV), C-O (286.4 eV), C=O (287.6 eV) and -COOH (289 eV) functional groups (**Fig. 2a**), while O1s spectra showed that oxygen content mostly in the form of organic carbon (at 533.45 and 532.12 eV). A peak at ~530.7 eV (O1s) indicated the presence of metal oxide in the composite [in the form of Fe_2O_3/Fe_3O_4 Fe(OH)O] and this might possible due to the oxidation of surface nZVI to Fe_2O_3/Fe_3O_4 and by the interaction with surface –COOH and –C=O group to form –COOFe/-OFe (**Fig. 2b**) [34-37]. Two intense peaks were observed for iron at ~711 eV (for 2p3/2) due to the formation of $Fe/Fe_2O_3/Fe_3O_4$/Fe(OH)O [34-37] and at ~725 eV (for 2p1/2) due to $FeOOH/Fe_2O_3$ (**Fig. 2c**) [38]. Thus, XPS results indicated that iron was successfully immobilized onto fBC surface which might form different species such as -BC-COO-Fe-OOC-BC, BC-O-Fe-O-BC, and BC-iron/ iron oxide particles. However, XRD result of nFe_3O_4-fBC after reaction with chloramphenicol only showed the presence of Fe_3O_4 in the composite (**Fig. 3a**) [39].

FTIR spectra of nZVI-fBC showed similar functional groups present on nZVI-fBC composite, with peaks at 3400-3800 cm^{-1} (–OH/-OFe-), ~1720 cm^{-1} (C=O), 1523-1595 cm^{-1}(C=C), and ~1020-2028 cm^{-1} (-COOH/-COOFe-) (**Fig. A3**). Additionally Raman spectroscopy was carried out to obtain deeper insight into the crystalline structure of the ZVI

and nZVI-fBC. Bare ZVI showed bands [10] at 215.7, 278, 392, 483, 590 cm^{-1} and maximum peak at 1282.5 cm^{-1} (**Fig. 3**). In the case of ZVI, the three peaks at ~215, ~278 and ~483 cm^{-1} were assigned to hematite. These results are well supported by Raman values reported for α-Fe_2O_3 in the literature [40]. A peak at ~394.7 cm^{-1} indicated both α-FeOOH and γ-FeOOH [41]. Another peat at ~483 cm^{-1} indicated α-FeOOH presence along with ZVI [41]. Raman spectra of nZVI-fBC showed three characteristic peaks at 1595.62, 1340.97 and 680 cm^{-1}. The two broad peaks located at 1340 cm^{-1} and 1595 cm^{-1} corresponded to the D-band and G-band of graphitic structures presence in nZVI-fBC. The band intensity ratio (I_G/I_D) showed the degree of functionalization in fBC. In addition, the peaks at ~680 cm^{-1} were due to the presence of magnetite Fe_3O_4 and FeO on the surface of nZVI-fBC [38, 40, 42, 43]. From literature, it is found that the Raman spectra of a freshly fractured Fe_3O_4 showed peaks at ~300, ~532 and ~661 cm^{-1} [40].

3.2. Application of nZVI for chloramphenicol reduction

nZVI was applied for the removal of chloramphenicol from different water types. nZVI could completely reduce 3.10 μM L^{-1} of chloramphenicol within ~5-6 h depending on the water types. No pronounced difference was observed in the complete reduction and dechlorination of chloramphenicol between different water types (**Fig. 4a**), although synthetic wastewater had slightly positive influence on the overall reduction of chloramphenicol followed by lake and deionized water. This is possibly due to the presence of different species that were favorable for the faster reduction of chloramphenicol in synthetic wastewater. In addition, species in synthetic wastewater might increase the ionic mobility of chloramphenicol towards nZVI particles resulted in strong interactions. However, lake water might contain less ionic species than synthetic wastewater but more than deionized water, resulting in moderate reduction of chloramphenicol. Furthermore, control experiments in the absence of nZVI with different water types showed that there was no loss of chloramphenicol. This indicated that

there was no adsorption/accumulation of chloramphenicol by organics present in synthetic wastewater.

The rate constant (k, min^{-1}) for chloramphenicol reduction was calculated using $C_t/C_o = e^{-kt}$, where C_o and C_t are chloramphenicol concentrations at time zero and any time, respectively. From the beginning to 3 h, the reduction rate of chloramphenicol by nZVI was fast possibly due to initial surface interactions [10]. The reduction nature of nZVI particles became slow with increasing time due to surface passivation of nZVI particles by reacting with surrounding environment. In terms of complete chloramphenicol reduction by nZVI particles, the reduction rate constant followed the order of deionized water < lake water < synthetic wastewater (**Table A4**). The detailed mechanism of chloramphenicol reduction by nZVI is presented in section 3.5.

3.3. nZVI-fBC application and its transformation to magnetic-fBC composite during chloramphenicol removal

nZVI-fBC composite showed simultaneous reduction and sorption in the 1st stage of application. Sorption was dominant over reduction and followed an opposite trend of nZVI i.e. deionized water > lake surface water > synthetic wastewater (**Fig. 4b**). As sorption was dominant over reduction, hence different organic and inorganic species in lake water and synthetic wastewater may interact with the fBC surface functional groups as well, competing with chloramphenicol; thus more time was needed than by nZVI for the complete removal of chloramphenicol. In the case of deionized water, there was no competitor of chloramphenicol, hence, sorption was faster. Initially, fast reduction of chloramphenicol using nZVI-fBC was observed by the loosely bonded surface nZVI following sorption by strongly bonded nZVI onto biochar surface. A small portion of loosely bonded surface nZVI was released into the solution during the application of nZVI-fBC composite in the 1st cycle. This was confirmed through the analysis of iron concentration in the supernatant by MP-AES and % Fe content on

the nZVI-fBC surface by EDS. From these results, it was found that 0.15% of iron content was lost from nZVI-fBC composite (initially 7.8%) and likely released into solution. The properties of nZVI-fBC composite were the main reason to take additional time than nZVI itself (~5-6 h, reduction was faster than sorption) and nZVI-fBC to be transformed into magnetic-fBC composite for complete removal of the same amount of chloramphenicol (**Fig. 4b**). Furthermore, in the 2nd cycle application of nZVI-fBC composite after transformation to magnetic-fBC, chloramphenicol reduction was negligible. Additionally no iron content was found in the solution. Thus the 2nd to 7th stage applications of nZVI-fBC showed that only sorption was dominant indicating that nZVI-fBC was transformed into magnetic biochar composite (i.e. nFe_3O_4-fBC). Some reactions might happen during the application and transformation of nZVI-fBC composite as proposed by Liu et al. [44]:

$$Fe^0 \text{ (in ZVI-fBC)} + 2H_2O \rightarrow Fe^{2+} + H_2 + 2OH^- \quad (2)$$

$$2Fe^0 + O_2 + 2H_2O \rightarrow 2Fe^{2+} + 4OH^- \quad (3)$$

$$6Fe^{2+} + O_2 + 6H_2O \rightarrow 2Fe_3O_4(s) + 12H^+ \quad (4)$$

FTIR spectra of nZVI-fBC after experiments shifted to lower absorbance peaks at 3400-3800 cm^{-1} (–OH/-OFe-), and at 1020 cm^{-1}(–COOH/-COOFe-) [32]. These might be due to the partial release of loosely bonded iron (-OFe/-COOFe or loosely bonded ZVI) from surface functional groups (-COOH/-OH) of fBC. Hence surface functional groups of fBC became free and showed lower absorbance at different positions (**Fig. A3**). EDS (**Table A1**) and MP-AES measurement already confirmed that after the 1st cycle application of nZVI-fBC, iron was released into the solution. Thus, during the first cycle, nZVI-fBC showed partial reduction followed by maximum sorption of chloramphenicol. As the sample was exposed to air during measurement, dissolved oxygen could cause partial oxidation of nZVI in nZVI-fBC composite forming iron oxygenated species (-COOFe-/-OFe/FeO/Fe_2O_3/Fe_3O_4) during the tests (**Figs 1d, 2b, and A4**) [28, 45]. Raman spectra of nZVI-fBC showed that band intensity ratio (I_G/I_D) increased after the application of nZVI-fBC composite in the 1st

cycle. This information clearly indicated that surface functional groups (C=O and C=C) in nZVI-fBC became free by participating in reduction process. Hence, surface ZVI (loosely bonded) and –COOFe- or –O-Fe- lost their iron content for the reduction of chloramphenicol due to the reaction with air (in particular dissolved oxygen). In addition, a stable peak for magnetite Fe_3O_4 at 673.3-685.2 cm^{-1} remained the same after experiment. From literature, it is found that the Raman spectra of fresh Fe_3O_4 showed peaks at ~300, ~532 and ~661 cm^{-1} [40]. Our XRD and magnetization test results after reaction also indicated the presence of magnetic Fe_3O_4 particles on the composite (**Fig. 3a**). Thereby, nZVI-fBC composite was fully transformed into magnetic-fBC (**equations 2 to 4**). In addition, in comparison with nZVI, nZVI-fBC composite material did not show any extra peaks like nZVI indicating no FeOOH, Fe_2O_3 i.e. hematite presence in the composite. However, C=O groups such as –COOH and -C=O might still associate with iron in the form of –COOFe- and C-O-Fe-. On the other hand, XPS spectra of O1s showed that the peak intensity of metal in oxide form (~530.6 eV), decreased to some extent which also indicated that loosely bonded iron took part in the reduction and stable metal oxide remained in the composite (**Figs 2b, 2c, A4b and A4c**). Moreover, Fe2p peak intensity also significantly decreased by forming some stable iron oxide. According to Tian et al. [38], the peaks at ~530.6 eV (for O1s), ~711 (for 2p3/2) and ~725 eV (for 2p1/2) were found before and after application indicating the presence of Fe_2O_3/ Fe_3O_4/Fe(OH)O in the composite (**Figs 2 and A4**). Besides, Raman spectra only indicated the presence of Fe_3O_4 and Fe(OH)O in the composite materials. Fe_3O_4 indicated the presence of magnetic particles in the composite while Fe(OH)O indicated the presence of iron species by forming bonds with the functional groups of fBC. The results showed that nZVI-fBC composite was transformed to stable magnetic (nFe_3O_4-fBC) composite during the application in the 1st cycle.

3.4. Comparative study among biochar, fBC, nFe_3O_4 and nFe_3O_4-fBC for chloramphenicol removal

Comparative study on the removal of chloramphenicol using biochar, nFe_3O_4-fBC, fBC and nFe_3O_4 was conducted to assess the synergistic effect. The results showed that nFe_3O_4 could remove only ~3.57% of chloramphenicol whereas biochar (eucalyptus biochar, 2.0 g L^{-1}) showed 57.5% removal (after 3 days of interactions). On the other hand, fBC and nFe_3O_4-fBC showed 100% removal. In addition, the sorption isotherm study showed that the maximum Langmuir sorption capacities were 258.95 μM $g^{-1}$and 406.77 μM g^{-1}, respectively for fBC and nFe_3O_4-fBC composite. The results indicated that transformed magnetic composite (nFe_3O_4-fBC) had synergistic effect with an increased sorption capacity of ~57% than fBC alone (**Fig. A5 and Table A5).**

3.5. Chloramphenicol reduction mechanisms and by-products

Fresh nZVI showed bands at 215.7, 278, 392, 483, 590 and 1282.5 cm^{-1}. The intensity of most of these peaks decreased significantly after reduction [10]. nZVI (nFe^o) showed maximum peak at ~1283 cm^{-1} and the peak intensity significantly decreased and slightly shifted to 1331.7 cm^{-1} at the end of the experiments. The result from the Raman spectra clearly indicated that nZVI particles took part in the reduction processes and peak intensity reduced significantly at different points (**Fig. 3**). Hematite (agglomerate particles), FeOOH and free nFe^o took part in the reduction process and the peak intensity was reduced significantly. This was also confirmed by the final solution pH being increased to ~8.6 from 4.0-4.5.

$$Fe^0 + H_2O \rightarrow Fe^{2+} + H_2 + OH^- \quad [5]$$

$$Fe^0 + R\text{-}Cl + H^+ \rightarrow Fe^{2+} + R\text{-}H + Cl^- \quad [6]$$

Again, when chloramphenicol interacted with nZVI and nZVI-fBC (1st cycle), amino group was formed rapidly by reducing nitro group due to release of electrons by nFe^0 and oxidized in the presence of water or dissolved oxygen (**reaction 5**) [46, 47]. Some of the

additional intermediates were quickly produced during reduction of nitro groups turned into firstly, nitroso (NO), secondly, hydroxylamino (HOAM) and thirdly, amine ($AMCl_2$) products of chloramphenicol (**Fig. 5**). In the second stage of reduction and dechlorination, $AMCl_2$ was transformed into two by-products namely 2-chloro-N-[1,3-dihydroxy-1-(4-aminophenyl)propan-2-yl]acetamide (1st product *m/z* 257) and dechlorinated N-[1,3-dihydroxy-1-(4-aminophenyl)propan-2-yl]acetamide (2nd product *m/z* 223) (**Reaction 6**, **Figs 6, A6 and 7**). The identification of by-products was confirmed using LC-MS-QTOF. During the first cycle application of nZVI-fBC, it was found that the loss of chloramphenicol was mostly due to reduction within first few hours and later stages once the surface of nZVI-fBC was transformed, the decrease in chloramphenicol concentration was mainly due to sorption onto nZVI-fBC surface. Moreover, negligible quantities of reduced products were detected in the solution after 18 h application of nZVI-fBC indicating that these by-products could have been sorbed by nFe_3O_4-fBC composite (**Fig. 7**). Furthermore, the 2nd cycle experiment showed minor reduction of chloramphenicol indicating that nZVI-fBC surface had been transformed to nFe_3O_4-fBC composite which gained only sorption properties (**Fig. A7**).

3.6. Mechanism of chloramphenicol sorption by nZVI-fBC and nFe_3O_4-fBC composite at pH 4.0-4.5

The removal ability of chloramphenicol by nZVI-fBC composite can be considered as two processes namely sorption (by both magnetic iron oxide and fBC) and reduction (by surface nZVI). The reduction mechanism has already been discussed in section 3.5. Chloramphenicol has hydrogen bond donors and acceptors groups according to its chemical structure. The application of nZVI-fBC composite was conducted at pH around 4.0-4.5 and the sorption mechanism can be discussed below. FTIR, Raman spectra, XPS and EDS analysis of nZVI-fBC confirmed the presence of different free functional groups (e.g. C=C, -COOH, -OH and π-π*) and iron particles (such as BC-COO-Fe-OOC-BC, BC-O-Fe-O-BC, fBC-iron/iron

oxide) (**Figs 2, 3, A3 and A4**). Chloramphenicol is non-ionisable compound and hydrolysis does not occur at pH 2-7 [48]. Thus, in the pH range of 4.0-4.5, proton exchange with water molecules is unfavourable (chloramphenicol + H_2O + fBC = Chloramphenicol$^+$ …fBC + OH^-) [32]. Generally, any carbonaceous surface -COOH group has pK_a value of ~3.0-5.0 [49, 50] and chloramphenicol has a pK_a value of ~5.5. So chloramphenicol could form hydrogen bonds at pH below 5.5 among fBC surface free functional groups (mostly –COOH) and nitro group present in chloramphenicol. This kind of chemical bonds are called charge assisted hydrogen bond (CAHB) **(c**hloramphenicol-NO_2 -----HOOC- BC**)**. Hydrogen bonds between surface carboxylic groups of fBC and hydroxyl groups in chloramphenicol also played a major role for the maximum sorption at this pH (chloramphenicol-OH-----HOOC-fBC**).** Strong electron donor-acceptor (EDA) interactions were favourable at the pH range 4.0-4.5 [51]. fBC surface is abundant with C=C aromatic carbon along with –OH groups (arene-OH) which can act as a π-electron donor (arene units as δ^- due to resonance effect of –OH groups), while chloramphenicol has nitro groups in its arene units which can act as π-electron acceptors (arene unit as δ^+ site in chloramphenicol due to resonance effect in the presence of sorbent) due to stronger EDA interactions (**Fig. A8**). Electron-acceptor-acceptor (EAA) interaction might also be possible between fBC surface free C=O groups (BC-C=O) and chloramphenicol arene units at this pH range although such interactions may not be strong. EAA interactions for –COOH/-COOFe- groups in fBC may not occur within this pH range as –COOH takes part in CAHB formation. Additionally, CAHB formation with surface hydroxyl groups (pK_a > 7.5) of biochar was not possible due to higher pK_a value. Moreover, based on Raman spectra, it was found that the G and D band peak intensity ratio (I_G/I_D) significantly decreased after sorption (**Fig. 3**). This clearly indicated strong interaction among surface functional groups and chloramphenicol molecules. FTIR peak shifted to a point where C=O (~1720 cm^{-1}) or –COOH functional groups (~1028 cm^{-1}) as well as –OH groups (3600-3800 cm^{-1}) locate due to the sorption of chloramphenicol onto biochar surfaces (**Fig. A3**) [52].

Thus, maximum sorption of chloramphenicol in this pH range was due to formation of CAHB and weak hydrogen bonds along with stronger EDA and EAA interactions in fBC surface free functional groups.

In addition, nZVI-fBC surface contains iron species in different forms such as BC-COO-Fe-OOC-BC, BC-O-Fe-O-BC and fBC-iron oxide particles. After application in the 1st stage, I_G/I_D ratio increased compared to initial nZVI-fBC implied that fBC functional groups became free and the intensity ratio increased (**Fig. 3**). XPS O1s spectra also indicated that stable magnetic Fe_3O_4 produced during the 1st cycle of application (**Fig. A4**). The results clearly implied that functional groups (-COOH/-OH/C=O) of fBC were distributed through different iron species on nZVI-fBC surface. Thus, sorption was fast through quick interaction of iron containing functional groups with nitro and hydroxyl functional groups of chloramphenicol. The formation of these bonds was stronger and faster compared to CAHB due to higher electron affinity of iron or iron oxides or, cation exchange capacity of iron towards chloramphenicol than carboxylic group hydrogen on biochar surface. Hence, sorption using nZVI-fBC required less time (~12 to 15 h) for the complete removal of the same amount of chloramphenicol. Separate experiments on the sorption of chloramphenicol using only fBC found that it took over 24 h for the complete sorption of the same amount of chloramphenicol at the same conditions. Further applications of this composite fully turned it into a stable magnetic-fBC composite, and sorption was accelerated due to formation of iron-oxide complex with chloramphenicol:

BC-COOFe-/-OFe- or, fBC-iron oxide → fBC-iron-oxygen complex (–NO_2 in chloramphenicol) or, BC-iron-hydroxyl complex (–OH in chloramphenicol) (7)

3.7. Percentage sorption and reduction of chloramphenicol and reusability of the materials

The amount of reduction and sorption of chloramphenicol using nZVI-fBC composite was calculated, with ~28% reduction and ~70% sorption for deionized water, ~32.5% reduction and ~67.5% sorption for synthetic wastewater, and ~31% reduction and ~69% sorption for lake water, respectively (**Fig. 8a**). The results clearly indicated that nZVI-fBC composite had simultaneous sorption and reduction capability. After 2nd cycle application of nFe_3O_4-fBC composite (nZVI-fBC transformed to nFe_3O_4-fBC), desorption amount increased significantly up to ~91.5%, ~90.9% and ~88.2% for deionized water, synthetic wastewater and lake water, respectively. These values confirmed that the application of nFe_3O_4-fBC composite from 2nd cycle onwards was solely due to sorption process (**Fig. A8**). Therefore, the reductive nature of nZVI-fBC composite was fully turned into sorptive nature from the transformation of nZVI-fBC to nFe_3O_4-fBC composite. Further sorption/desorption experiments confirmed that the nFe_3O_4-fBC composite can be regenerated thermally in a repetitive manner up to six cycles, can maintain excellent reusability with ~100% chloramphenicol removal up to > 6 cycles of applications (**Fig. 8b**).

3.8. Application of nFe_3O_4-fBC composite to remove methylene blue

After six cycles of application for the removal of chloramphenicol, the nFe_3O_4-fBC composite was used for the sorption of methylene blue. The results indicated that the magnetic composite took ~90 min, ~140 min and ~210 min for the complete removal of 2.5, 5.0 and 10.0 mg L^{-1} methylene blue, respectively. In addition, the maximum Langmuir sorption capacity of nFe_3O_4-fBC composite for sorption of methylene blue was found to be 285.25 mg g^{-1} with high R^2 (0.981). Maximum Freundlich sorption constant value was found to be 82.06 $mg^{1-n} L^n g^{-1}$ (**Fig. A9**). The sorption capacity was higher than reported values of 64.7-270 mg g^{-1} using different carbon materials such as activated carbon, graphene and carbon nanotube [53-55]. Thus, nFe_3O_4-fBC composite showed high sorption capability of methylene blue even after six cycles of application in chloramphenicol removal.

4. Conclusions

The interactions of nZVI and nZVI-fBC composite with chloramphenicol were very effective even in different water types. nZVI showed fast reduction capability. Although successfully immobilized, the nZVI-fBC composite quickly changed into magnetic-biochar composite (nFe_3O_4-fBC) during the 1st stage of application, within a few hours, possessing simultaneous reduction (29-32.5%) and sorption (67.5-70.5%) capabilities. Further interactions leading to sorptive behavior of newly formed nFe_3O_4-fBC composite and sorption had accelerated to next stage of applications with synergistic effect for chloramphenicol than fBC only. The removal of chloramphenicol was almost similar with different water types. Thermal regeneration of the magnetic composite showed excellent performance up to seven cycles, which can further remove methylene blue subsequently. Therefore, the results demonstrate further research is needed on nZVI immobilization onto biochar due to the instability of the immobilized nZVI-fBC composite. Overall, the transformed magnetized composite can serve as a powerful sorbent for chloramphenicol, methylene blue and other similar organic contaminants from water and wastewater.

Conflict of financial interest

Authors declare no competing financial interest.

Acknowledgements

This research was funded by a Blue Sky Seed Fund (2232137) from the Faculty of Engineering and Information Technology, University of Technology Sydney. Special thanks to New Forest Asset Management Pty Ltd, Portland, Victoria, Australia for donating *Eucalyptus Globulus* wood sample.

References

[1] I. Dror, O. M. Jacov, A. Cortis, B. Berkowitz, Catalytic transformation of persistent contaminants using a new composite material based on nanosized zero-valent iron, ACS Appl. Mater. Interfaces 4 (2012), 3416-3423.

[2] H. Sun, G. Zhou, S. Liu, H.M. Ang, M.O. Tadé, S. Wang, Nano-Fe^0 encapsulated in microcarbon spheres: synthesis, characterization, and environmental applications, ACS Appl. Mater. Interfaces 4 (2012), 6235-6241.

[3] M. Liu, Y. Wang, L. Chen, Y. Zhang, Z. Lin, $Mg(OH)_2$ supported nanoscale zero valent iron enhancing the removal of Pb (II) from aqueous solution, ACS Appl. Mater. Interfaces 7(2015), 7961-7969.

[4] H. Khalil, D. Mahajan, M. Rafailovich, M. Gelfer, K. Pandya, Synthesis of zerovalent nanophase metal particles stabilized with poly (ethylene glycol), Langmuir 20 (2004), 6896-6903.

[5] F. Fu, D.D. Dionysiou, H. Liu, The use of zero-valent iron for groundwater remediation and wastewater treatment: a review, J. Hazard. Mater. 267 (2014), 194-205.

[6] B. Sunkara, J. Zhan, J. He, G.L. McPherson, G. Piringer, V.T. John, Nanoscale zerovalent iron supported on uniform carbon microspheres for the in situ remediation of chlorinated hydrocarbons, ACS Appl. Mater. Interfaces 2 (2010), 2854-2862.

[7] Y.P. Sun, X.Q. Li, J. Cao, W.X. Zhang, H.P. Wang, Characterization of zero-valent iron nanoparticles, Adv. Colloid Interface Sci. 120 (2006), 47-56.

[8] J. Xu, X. Liu, G.V. Lowry, Z. Cao, H. Zhao, J.L. Zhou, X. Xu, Dechlorination mechanism of 2,4-dichlorophenol by magnetic MWCNTs supported Pd/Fe nanohybrids: rapid adsorption, gradual dechlorination, and desorption of phenol, ACS Appl. Mater. Interfaces 8 (2016), 7333-7342.

[9] M. Nie, C. Yan, M. Li, X. Wang, W. Bi, W. Dong, Degradation of chloramphenicol by persulfate activated by Fe^{2+} and zerovalent iron, Chem. Eng. J. 279 (2015), 507-515.

[10] S. Xia, Z. Gu, Z. Zhang, J. Zhang, S.W. Hermanowicz, Removal of chloramphenicol from aqueous solution by nanoscale zero-valent iron particles, Chem. Eng. J. 257 (2016), 98-104.

[11] W. Chu, S. Ding, T. Bond, N. Gao, D. Yin, B. Xu, Z. Cao, Zero valent iron produces dichloroacetamide from chloramphenicol antibiotics in the absence of chlorine and chloramines, Water Res. 104 (2016), 254-261.

[12] Y. Zou, X. Wang, A. Khan, P. Wang, Y. Liu, A. Alsaedi, X. Wang, Environmental remediation and application of nanoscale zero-valent iron and its composites for the removal of heavy metal ions: a review, Environ. Sci. Technol. 50 (2016), 7290-7304.

[13] S. Wang, B. Gao, Y. Li, A.E. Creamer, F. He, Adsorptive removal of arsenate from aqueous solutions by biochar supported zero-valent iron nanocomposite: Batch and continuous flow tests, J. Hazard. Mater. 322 (2017), 172-181.

[14] J.N. Xiao, B.Y. Gao, Q.Y. Yue, Y. Y. Sun, J.J. Kong, Y. Gao, Q. Li, Characterization of nanoscale zero-valent iron supported on granular activated carbon and its application in removal of acrylonitrile from aqueous solution, J. Taiwan Inst. Chem. Eng. 55 (2015), 152−158.

[15] J.N. Xiao, B.Y. Gao, Q.Y. Yue, Y. Gao, Q. Li, Removal of trihalomethanes from reclaimed-water by original and modified nanoscale zero-valent iron: characterization, kinetics and mechanism, Chem. Eng. J. 262 (2015), 1226−1236.

[16] G. D. Sheng, A. Alsaedi,W. Shammakh, S. Monaquel, J. Sheng, X.K. Wang, H. Li, Y.Y. Huang, Enhanced sequestration of selenite in water by nanoscale zero valent iron immobilization on carbon nanotubes by a combined batch, XPS and XAFS investigation, Carbon 99 (2016), 123−130.

[17] C. Üzüm, T. Shahwan, A.E. Eroglu, K.R. Hallam, T.B. Scott, I. Lieberwirth, Synthesis and characterization of kaolinite-supported zero-valent iron nanoparticles and their

application for the removal of aqueous Cu^{2+} and Co^{2+} ions, Appl. Clay Sci. 43 (2009), 172–181.

[18] S.A. Kim, S.K. Kannan, K.J. Lee, Y.J. Park, P.J. Shea, W.H. Lee, H.M. Kim, B.T. Oh, Removal of Pb(II) from aqueous solution by a zeolite-nanoscale zero-valent iron composite, Chem. Eng. J. 217 (2013), 54–60.

[19] S. Bhowmick, S. Chakraborty, P. Mondal, W.V. Renterghem, S.V. D. Berghe, G.R. Ross, D. Chatterjee, M. Iglesias, Montmorillonite-supported nanoscale zero-valent iron for removal of arsenic from aqueous solution: kinetics and mechanism, Chem. Eng. J. 243 (2014), 14–23.

[20] N. Yuan, G. Zhang, S. Guo, Z. Wan, Enhanced ultrasoundassisted degradation of methyl orange and metronidazole by rectoritesupported nanoscale zero-valent iron, Ultrason. Sonochem. 28 (2016), 62–68.

[21] Z.X. Chen, X.Y. Jin, Z. Chen, M. Megharaj, R. Naidu, Removal of methyl orange from aqueous solution using bentonite-supported nanoscale zero-valent iron, J. Colloid Interface Sci. 363 (2011), 601–607.

[22] Y.M. Li, W. Cheng, G.D. Sheng, J.F. Li, H.P. Dong, Y. Chen, L.Z. Zhu, Synergetic effect of a pillared bentonite support on SE(VI) removal by nanoscale zero valent iron, Appl. Catal. B. 147-175 (2015), 329–335.

[23] J. Fatisson, S. Ghoshal, N. Tufenkji, Deposition of carboxymethylcellulose-coated zero-valent iron nanoparticles onto silica: roles of solution chemistry and organic molecules. Langmuir (2010), 12832-12840.

[24] M.B. Ahmed, J.L. Zhou, H.H. Ngo, W. Guo, Adsorptive removal of antibiotics from water and wastewater: Progress and challenges, Sci. Total Environ. 53 (2015), 112-126.

[25] M.B. Ahmed, J.L. Zhou, H.H. Ngo, W. Guo, N.S. Thomaidis, J. Xu, Progress in the biological and chemical treatment technologies for emerging contaminant removal from wastewater: a critical review, J. Hazard. Mater. 323 (2017), 274-298.

[26] P. Liao, Z. Zhan, J. Dai, X. Wu, W. Zhang, K. Wang, S. Yuan, Adsorption of tetracycline and chloramphenicol in aqueous solutions by bamboo charcoal: a batch and fixed-bed column study, Chem. Eng. J. 228 (2013), 496-505.

[27] C.Q. Chen, L. Zheng, J.L. Zhou, H. Zhao, Persistence and risk of antibiotic residues and antibiotic resistance genes in major mariculture sites in Southeast China. Sci. Total Environ. 580 (2017), 1175-1184

[28] W. Guo, M. Geng, H. Song, J. Sun, Removal of chloramphenicol and simultaneous electricity generation by using microbial fuel cell technology, Int. J. Electrochem. Sci. 11 (2016), 5128-5139.

[29] K. Chen, J.L. Zhou, Occurrence and behavior of antibiotics in water and sediments from the Huangpu River, Shanghai, China, Chemosphere 95 (2014), 604-612.

[30] D. Wu, Y. Chen, Z. Zhang, Y. Feng, Y. Liu, J. Fan, Y. Zhang, Enhanced oxidation of chloramphenicol by GLDA-driven pyrite induced heterogeneous Fenton-like reactions at alkaline condition, Chem. Eng. J. 294 (2016), 49-57.

[31] G. Lofrano, G. Libralato, R. Adinolfi, A. Siciliano, P. Iannece, M. Guida, M. Giugni, A. V. Ghirardini, M. Crotenuto, Photocatalytic degradation of the antibiotic chloramphenicol and effluent toxicity effects, Ecotox. Environ. Safe. 123 (2016), 65-71.

[32] M.B. Ahmed, J.L. Zhou, H.H. Ngo, W. Guo, M.A.H. Johir, K. Sornalingam, Single and competitive sorption properties and mechanism of functionalized biochar for removing sulfonamide antibiotics from water, Chem. Eng. J. 311 (2017), 348-358.

[33] M. Johir, M. Pradhan, P. Loganathan, J. Kandasamy, S. Vigneswaran, Phosphate adsorption from wastewater using zirconium (IV) hydroxide: kinetics, thermodynamics and membrane filtration adsorption hybrid system studies, J. Environ. Manage. 167 (2016), 167-174.

[34] R. Li, Y. Wang, C. Zhou, C. Wang, X. Ba, Y. Li, J. Liu, Carbon-stabilized high-capacity ferroferric oxide nanorod array for flexible solid-state alkaline battery–supercapacitor

hybrid device with high environmental suitability, Adv. Funct. Mater. 25 (2015), 5384-5394.

[35] X. Qiu, Z. Fang, B. Liang, F. Gu, Z. Xu, Degradation of decabromodiphenyl ether by nano zero-valent iron immobilized in mesoporous silica microspheres, J. Hazard. Mater. 193 (2011), 70-81.

[36] Ç.Üzüm, T. Shahwan, A.E. Eroğlu, I. Lieberwirth, T.B. Scott, K.R. Hallam, Application of zero-valent iron nanoparticles for the removal of aqueous Co^{2+} ions under various experimental conditions, Chem. Eng. J. 144 (2008), 213-220.

[37] C.T. Wu, K.M.K. Yu, Y. Liao, N. Young, P. Nellist, A. Dent, S.C.E. Tsang, A non-syn-gas catalytic route to methanol production, Nat. Commun. 3 (2012), 1050.

[38] Q. Tian, Q. Wang, Q. Xie, J. Li, Aqueous solution preparation, structure, and magnetic properties of nano-granular Zn_x $Fe_{3-x}O_4$ ferrite films, Nanoscale Res. Lett. 5 (2010), 1518.

[39] X. Zhang, Y. Niu, X. Meng, Y. Li, J. Zhao, Structural evolution and characteristics of the phase transformations between α-Fe_2O_3, Fe_3O_4 and γ-Fe_2O_3 nanoparticles under reducing and oxidizing atmospheres. CrystEngComm. 15 (2013), 8166-8172.

[40] D.L.A. De Faria, S. Venâncio Silva, M.T. De Oliveira, Raman microspectroscopy of some iron oxides and oxyhydroxides, J. Raman Spectrosc. 28 (1997), 873-878.

[41] D.K. Padhi, K. Parida, Facile fabrication of α-FeOOH nanorod/RGO composite: a robust photocatalyst for reduction of Cr(VI) under visible light irradiation, J. Mater. Chem. A 2 (2014), 10300-10312.

[42] C. Ban, Z. Wu, D.T. Gillaspie, L. Chen, Y. Yan, J.L. Blackburn, A.C. Dillon, Nanostructured Fe_3O_4/SWNT electrode: binder-free and high-rate Li-ion anode, Adv. Mater. 22 (2010), E145-E149.

[43] C. Wang, G. Shao, Z. Ma, S. Liu, W. Song, J. Song, Constructing Fe_3O_4@ N-rich carbon core-shell microspheres as anode for lithium ion batteries with enhanced electrochemical performance, Electrochim. Acta. 130 (2014), 679-688.

[44] A. Liu, J. Liu, J. Han, W. X. Zhang, Evolution of nanoscale zero-valent iron (nZVI) in water: Microscopic and spectroscopic evidence on the formation of nano-and micro-structured iron oxides, J. Hazard. Mater. 322 (2017), 129-135.

[45] J. A. Mielczarski, G.M. Atenas, E. Mielczarski, Role of iron surface oxidation layers in decomposition of azo-dye water pollutants in weak acidic solutions, Appl. Catal. B. Environ. 56 (2005), 289-303.

[46] B. Liang, H.Y. Cheng, D.Y. Kong, S.H. Gao, F. Sun, D. Cui, F.Y. Kong, A.J. Zhou, W.Z. Liu, N.Q. Ren, Accelerated reduction of chlorinated nitroaromatic antibiotic chloramphenicol by biocathode, Environ. Sci. Technol. 47 (2013), 5353-5361.

[47] Y.C. Huo, W.W. Li, D. Min, D.D. Wang, H.Q. Liu, Q. Kong, R.J. Zeng, Zero-valent iron nanoparticles with sustained high reductive activity for carbon tetrachloride dechlorination, RSC Adv. 5 (2015), 54497-54504.

[48] T. Higuchi, A.D. Marcus, The kinetics of degradation of chloramphenicol in solution: III. The nature, specific hydrogen ion catalysis, and temperature dependencies of the degradative reactions, J. Am. Pharm. Assoc. 43 (1954), 530-535.

[49] M. Teixidó, J.J. Pignatello, J.L. Beltrán, M. Granados, J. Peccia, Speciation of the ionizable antibiotic sulfamethazine on black carbon (biochar), Environ. Sci. Technol. 45 (2011), 10020-10027.

[50] B. Pan, B. Xing, Adsorption mechanisms of organic chemicals on carbon nanotubes, Environ. Sci. Technol. 42 (2008), 9005-9013.

[51] Y. Fan, B. Wang, S. Yuan, X. Wu, J. Chen, L. Wang, Adsorptive removal of chloramphenicol from wastewater by NaOH modified bamboo charcoal, Bioresour. Technol. 101 (2010), 7661-7664.

[52] M.B. Ahmed, J.L. Zhou, H.H. Ngo, W. Guo, M. Chen, Progress in the preparation and application of modified biochar for improved contaminant removal from water and wastewater, Bioresour. Technol. 214 (2016), 836-851.

[53] Y. Li, Q. Du, T. Liu, X. Peng, J. Wang, J. Sun, Y. Wang, S. Wu, Z. Wang, Y. Xia, L. Xia, Comparative study of methylene blue dye adsorption onto activated carbon, graphene oxide, and carbon nanotubes. Chem. Eng. Res. Des. 91(2013), 361-368.

[54] Y. Yao, F. Xu, M. Chen, Z. Xu, Z. Zhu, Adsorption behavior of methylene blue on carbon nanotubes. Bioresour. Technol. 101(2010), 3040-3046.

[55] T. Liu, Y. Li, Q. Du, J. Sun, Y. Jiao, G. Yang, Z. Wang, Y. Xia, W. Zhang, K. Wang, H. Zhu, Adsorption of methylene blue from aqueous solution by graphene. Colloids Surf. B Biointerface. 90 (2012), 197-203.

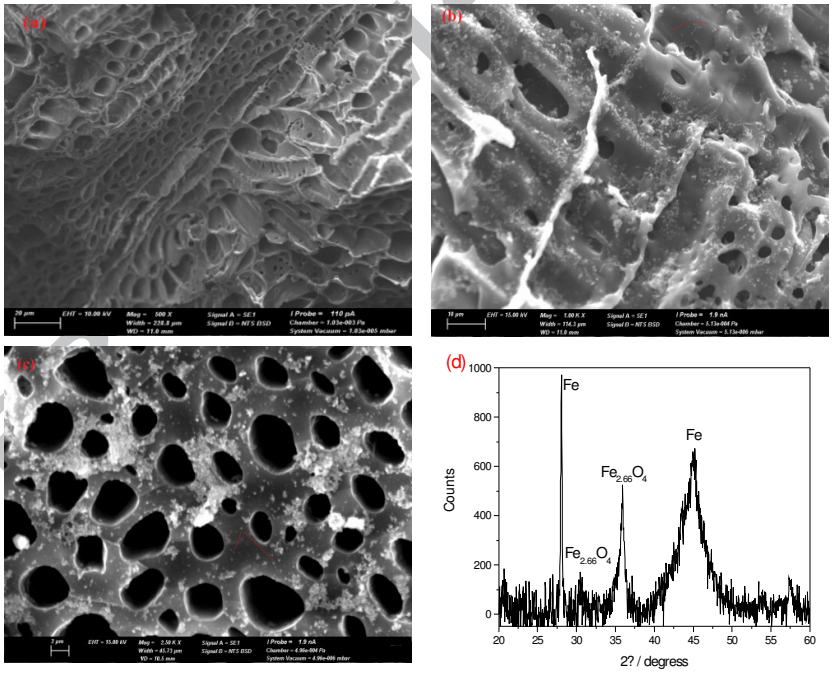

Figure 1. SEM cross-sectional images of fBC, nZVI-fBC and nFe_3O_4-fBC composite (after application of nZVI-fBC), respectively (**a-c**) using scanning electron microscope (SEM) with energy dispersive spectrometer (EDS) and XRD pattern of nZVI (**d**).

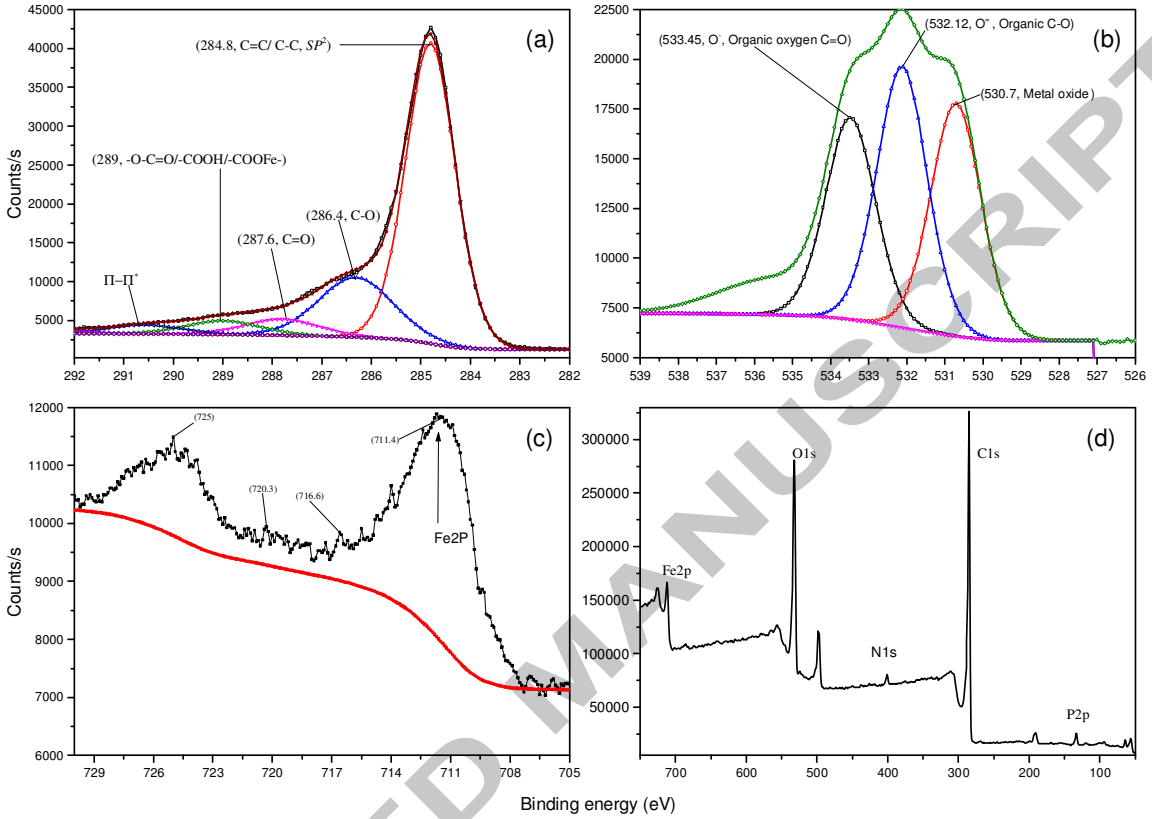

Figure 2. XPS analysis of nZVI-fBC composite before sorption experiments. Spectra were obtained by plotting counts against binding energy for C1s (**a**), O1s (**b**), Fe2p (**c**) and overall survey (**d**) in a wide scan.

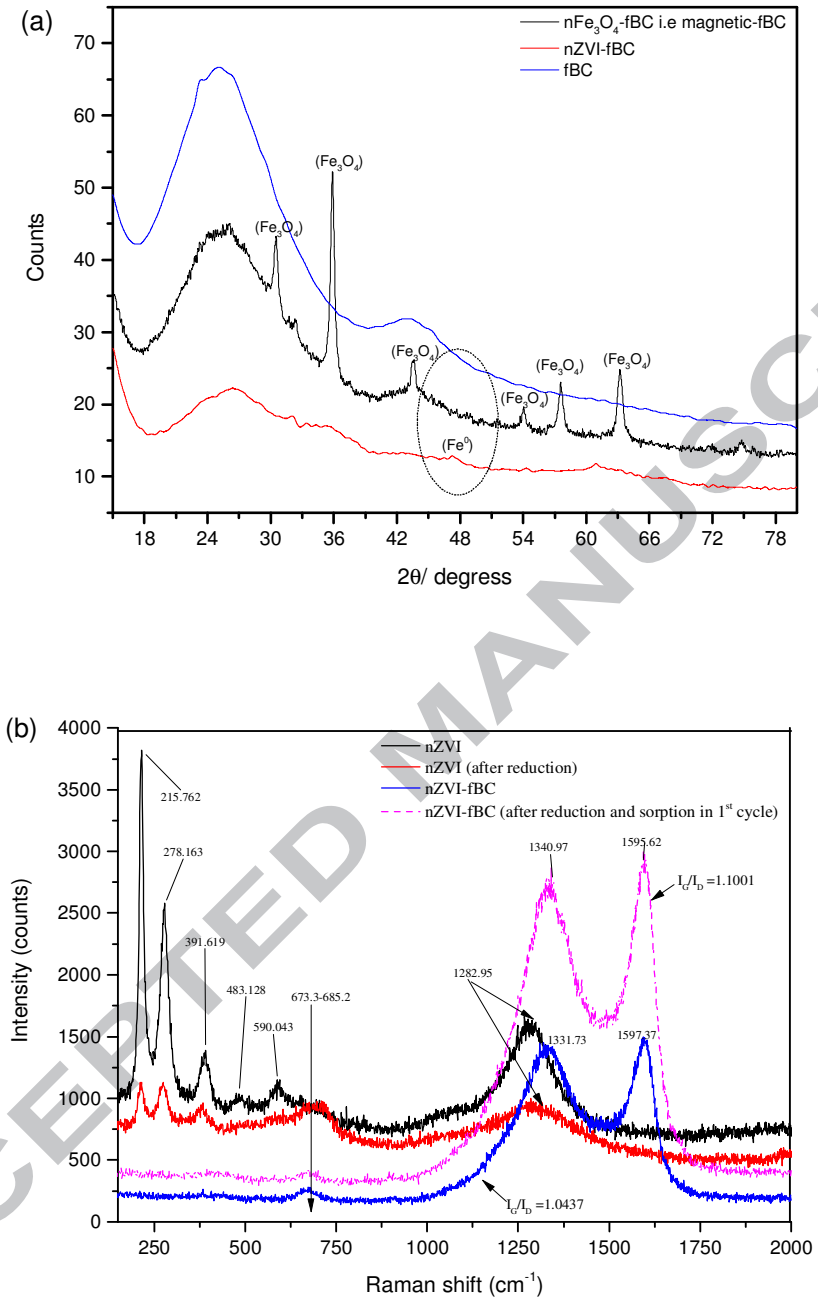

Figure 3. XRD pattern of fBC, nZVI-fBC and nFe_3O_4-fBC (a). Raman spectra of nZVI and nZVI-fBC composite (with band ratio, I_G/I_D) for the removal of chloramphenicol before and after experiments (b).

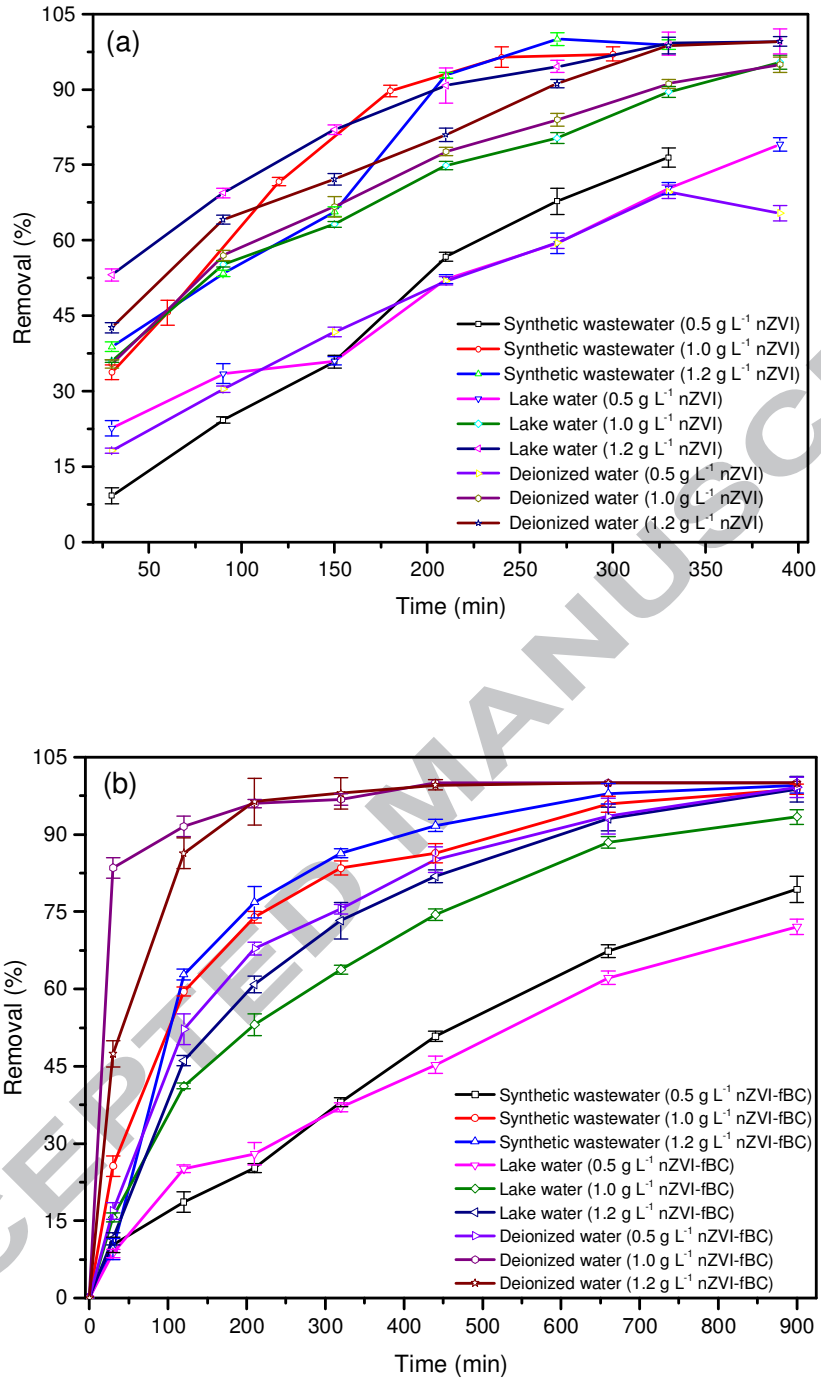

Figure 4. Percentage removal (±standard deviation) of chloramphenicol with time using nZVI (a) and nZVI-fBC composite (b). The initial concentration of chloramphenicol was 3.10 μM L^{-1}, pH 4.0-4.5, 25 °C from different water matrices with different dosages of nZVI and nZVI-fBC composite.

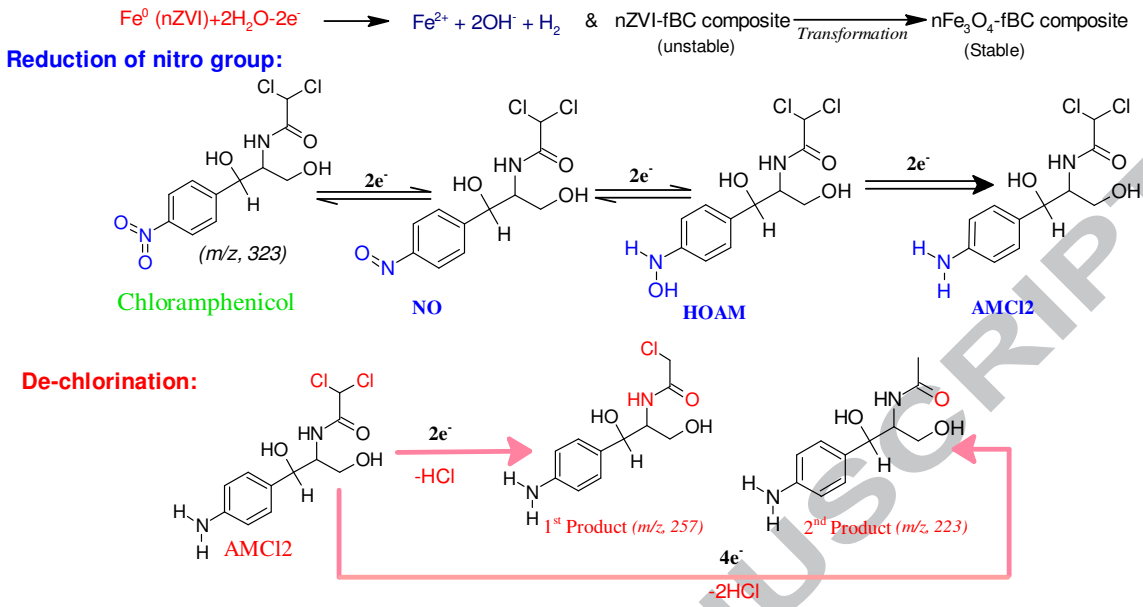

Figure 5. Proposed reduction and dechlorination mechanisms for the removal of chloramphenicol from water and wastewater.

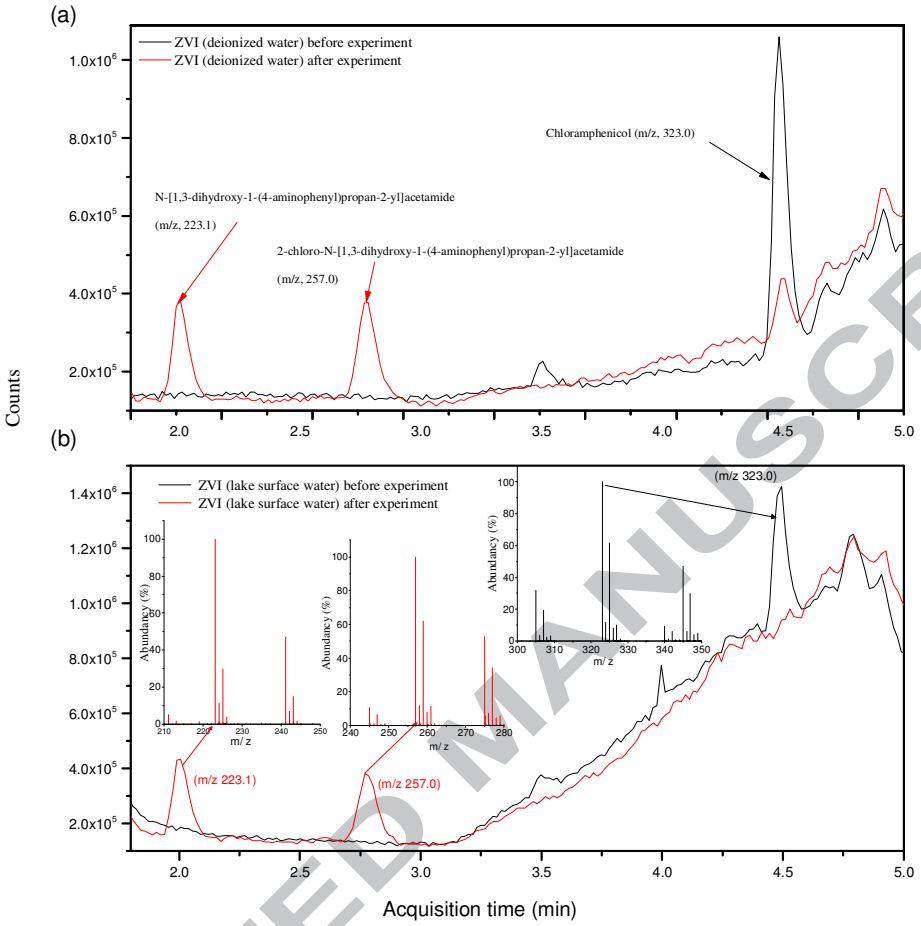

Figure 6. Chloramphenicol transformation by-products identified by their retention times (2.1 min, 2.7 min) in LC and mass spectra by LC-MS/QTOF from deionized water (**a**) and lake water (**b**) using nZVI only (sample collected after 8 h). LC-MS/QTOF method run for 13 min and data plotted up to 5 min.

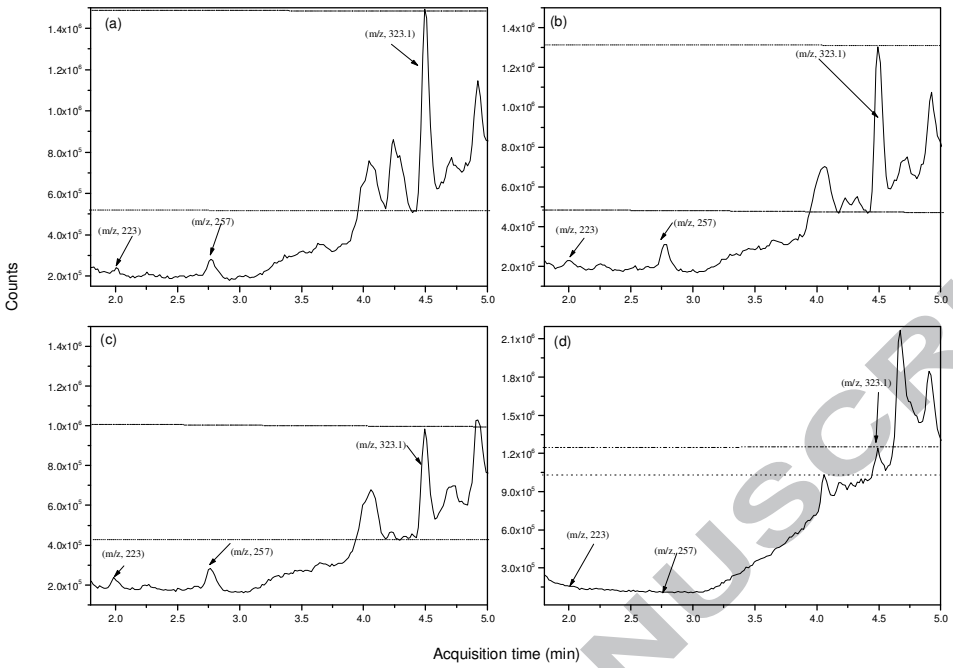

Figure 7. Chloramphenicol transformation products highlighted by their retention times after 10 min (**a**), 30 min (**b**), 150 min (**c**), and 12 h (**d**) using nZVI-fBC in synthetic wastewater during the 1st cycle application. LC-MS/QTOF method run for 13 min and data plotted up to 5 min.

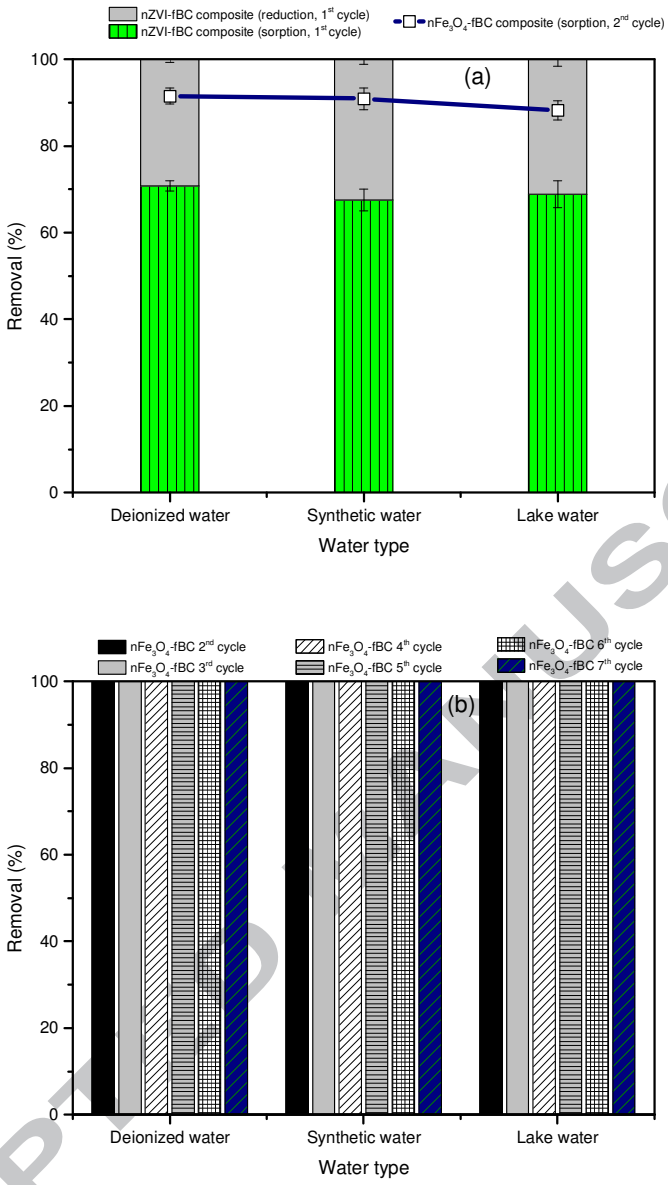

Figure 8. Percentage of sorption and reduction (cumulative basis, after excluding the amount of recoverable chloramphenicol) using nZVI-fBC composite (in the 1st cycle) followed by sorption only onto nFe_3O_4-fBC composite (**a).** Reusability of nFe_3O_4-fBC composite for the repetitive applications (up to 7 cycles) for the removal of chloramphenicol (3.10 μM L^{-1} initial concentration) at pH 4.0-4.5, 25 °C from different water **(b)**.

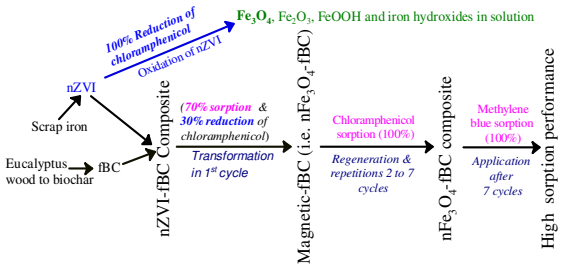

Highlights

- nZVI was synthesized and immobilized to produce nZVI-fBC composite.
- nZVI-fBC simultaneously reduced (~30%) and sorbed (~70%) chloramphenicol.
- nZVI-fBC transformed to stable nFe_3O_4-fBC composite.
- nFe_3O_4-fBC composite showed excellent reusability with synergistic effect.
- nFe_3O_4-fBC showed excellent performance to remove methylene blue.